Optical control of TRPV1 channels *in vitro* with tethered photopharmacology

Carmel L. Howe[a,#], David Icka-Araki[a,#], James A. Frank[a,b*]

[a] Department of Chemical Physiology and Biochemistry, Oregon Health & Science University, Portland, OR, USA. [b] Vollum Institute, Oregon Health & Science University, Portland, OR, USA

[#]Co-first authors
*Correspondence should be addressed to: frankja@ohsu.edu

ABSTRACT

Transient receptor potential vanilloid 1 (TRPV1) is a nonselective cation channel that is important for nociception and inflammatory pain, and is activated by a variety of nociceptive stimuli—including lipids such as capsaicin (CAP) and endocannabinoids. TRPV1's role in physiological systems is often studied by activating it with externally perfused ligands; however, this approach is plagued by poor spatiotemporal resolution. Lipid agonists are insoluble in physiological buffers and can permeate membranes to accumulate non-selectively inside cells, where they have off-target effects. To increase the spatiotemporal precision with which we can activate lipids on cells and tissues, we previously developed Optically-Cleavable Targeted (OCT)-ligands, which use protein tags (SNAP-tags) to localize a photocaged ligand on a target cellular membrane. After enrichment, the active ligand is released on a flash of light to activate nearby receptors. In this work, we expand the scope of OCT-ligand technology to target TRPV1. We synthesize a probe, OCT-CAP, that tethers to membrane-bound SNAP-tags and releases a TRPV1 agonist when triggered by UV-A irradiation. Using Ca^{2+} imaging and electrophysiology in HEK293T cells expressing TRPV1, we demonstrate that OCT-CAP uncaging activates TRPV1 with superior spatiotemporal precision when compared to standard diffusible ligands or photocages. This study demonstrates the versatility of OCT-ligands to manipulate ion-channel targets, and we anticipate that these tools will find many applications in controlling lipid signaling pathways in various cells and tissues.

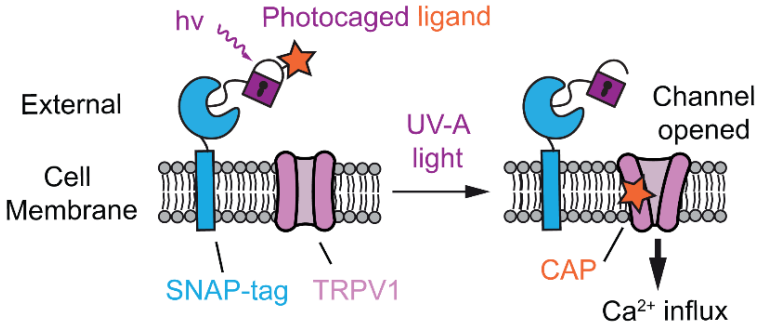

INTRODUCTION

The transient receptor potential vanilloid 1 (TRPV1) ion channel is a nonselective cation channel that is important for nociception, and has received considerable attention as a drug target for pain and inflammation[1,2]. TRPV1 is expressed in sub-populations of sensory neurons within the trigeminal and dorsal root ganglia, brain regions like the hippocampus[3,4], and in non-neuronal cells, such as pancreatic β-cells[5]. TRPV1 responds to a variety of chemical and physical stimuli: including noxious heat (<43 °C), peptide toxins/poisons[6,7], and acidic extracellular pH[8]. Notably, TRPV1 is also activated by a set of amide lipids—including capsaicin (CAP) and the endocannabinoid anandamide[9]—which are often externally applied by perfusion to activate TRPV1 in physiological studies. However, TRPV1 pharmacology is plagued by poor spatiotemporal resolution due to the hydrophobic nature of TRPV1's lipid agonists, which clouds our understanding of TRPV1 physiology in heterogeneous tissues. Lipids can cross membranes and accumulate non-selectively in intracellular compartments, where they can have off-target effects. Additionally, their insolubility in physiological solutions complicates drug handling procedures, and makes drug activation kinetics inconsistent due to competing TRPV1 desensitization. To better understand the function of TRPV1 and its ligands in complex biological systems, new tools are needed to activate TRPV1 with enhanced spatiotemporal control.

Small molecules whose biological activity (efficacy) can be fine-tuned with light offer a solution to the limited precision of standard pharmacology. Coined *photopharmacology*, this approach allows ligands, and consequently their endogenous receptors and downstream pathways, to be activated on-demand using light as the trigger[10]. Photopharmacology probes can incorporate either photoswitches or light sensitive protecting groups, called photocages. Our group and others have developed photoswitchable ligands for TRPV1 that contain an azobenzene photoswitch. These enable reversible, optical control over membrane potential and Ca^{2+} influx in TRPV1-expressing cells[11–13], and have even been applied *in vivo*[14]. However, the photoswitchable ligand approach is unable to truly represent endogenous or natural TRPV1 ligands, because the photoswitch always remains attached to the molecule. To this end, photocaged probes, which contain a photo-labile protecting group that blocks the ligand's activity[15], have been developed[16–20]. Photocages are inactive until exposed to light, when they irreversibly release the unmodified ligand to bind nearby receptors. Advantageously, photocages allow for endogenous molecules to be released on-demand[21]. However, a disadvantage to both conventional photoswitches and photocages is that they are still free to

diffuse throughout the cells or tissue. These probes cannot be genetically targeted to specific cells or membranes, which is a key property driving the utility of chemogenetic and optogenetic technologies that remain the gold standard for manipulating cell signaling in complex living systems[22–24].

To increase the spatial precision of photopharmacology, light-sensitive ligands can be targeted to cellular membranes or proteins of interest using a biorthogonal self-labeling protein-tags—such as SNAP-[25], Halo-[26,27], or CLIP-tags[28]. Our group recently developed the Optically-Cleavable Targeted (OCT)-ligand approach[29], where a photocaged ligand is enriched through SNAP-tag bioconjugation, and then released with a flash of light to activate nearby receptors. Our proof-of-concept work presented an OCT-ligand to release the endocannabinoid palmitoylethanolamide, which was uncaged on the surface of a pancreatic β-cell line to modulate intracellular Ca^{2+} levels through an endocannabinoid-sensitive GPCR. While OCT-ligand technology promises the ability to target endogenous signaling pathways at genetically-defined locations in cells and tissue, it remained limited in scope and had yet to be applied to control other ligands or biological targets, such as ion channels.

Herein, we report the expansion of OCT-ligand technology to target TRPV1. We synthesized a probe, OCT-CAP, which contains a photocaged TRPV1 agonist that can be enriched on genetically-defined cellular membranes by SNAP-tag tethering, then UV-A illumination releases the ligand to activate nearby TRPV1 channels. Using Ca^{2+} imaging and electrophysiology in HEK293T cells expressing TRPV1, we demonstrate that OCT-CAP uncaging on the cell surface activates TRPV1 with superior spatiotemporal precision when compared to standard bath application of diffusible ligands or photocages. More broadly, this work presents the first example of OCT-ligands targeting ion channels, and sets the stage for their wider application to manipulate diverse biological targets.

RESULTS

Design and synthesis of an OCT-ligand targeting TRPV1

We designed an OCT-ligand to target TRPV1—coined OCT-CAP (**Figure 1A**)—which contains the TRPV1 agonist (orange), a photocage (purple), linker (black), and bioconjugation motif (blue) (**Figure 1B**). Dihydrocapsaicin, which lacks the *trans*-double bond on the CAP acyl chain, was selected as the TRPV1 agonist due to its synthetic accessibility and comparable TRPV1 potency to CAP[30,31]. Dihydrocapsaicin's potency was blocked through the formation of a tertiary amide bond, which connects to the benzylic position of an ortho-nitrobenzyl (oNB) photocage. The use of an oNB cage was necessary due to the amide bond being a poor leaving group. The distal end of the photocage is connected via triazole to a short polyethylene glycol chain, that links to an O^6-(4-aminomethyl-benzyl)guanine (BG) motif. The BG allows the probe to be covalently tethered to SNAP-tags at cysteine residue C145.

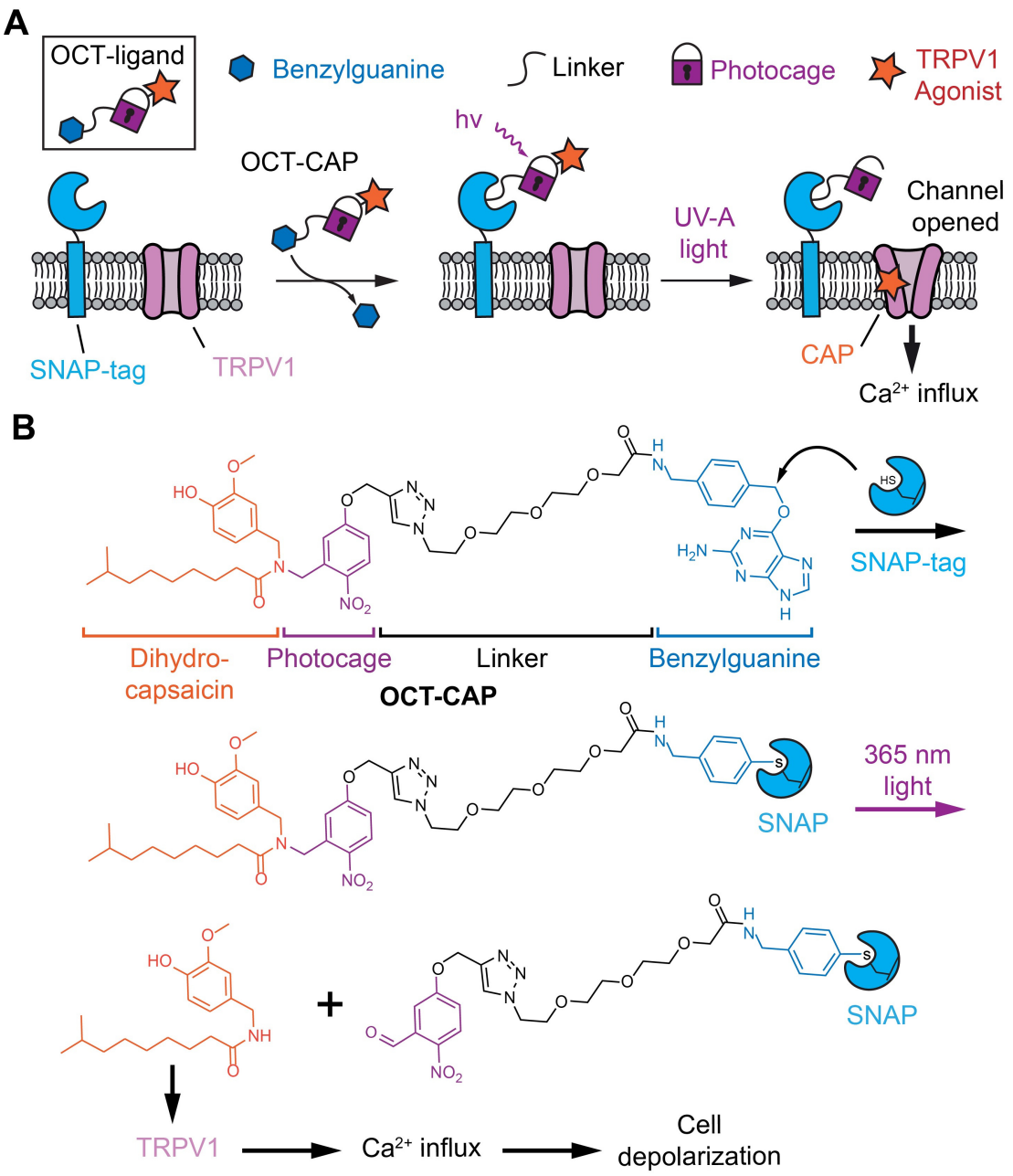

Figure 1. Design of an OCT-ligand to target endogenous TRPV1 channels. (**A**) Schematic depiction of the OCT-ligand approach. A photocaged TRPV1 agonist is localized to cell membranes at the site of SNAP-tag expression. UV-A illumination releases an agonist to open nearby TRPV1 ion channels. (**B**) Molecular structure of OCT-CAP, which consists of the TRPV1 agonist, dihydrocapsaicin (orange), masked as a tertiary amide with a nitrobenzyl photocage (purple). The distal end of the photocage is linked to a BG motif for SNAP-tag tethering (blue). Photolysis using 365 nm light releases dihydrocapsaicin to activate nearby TRPV1 channels.

OCT-CAP was synthesized from commercially available 5-Hydroxy-2-nitrobenzaldehyde in six steps and 27% overall yield (**Figure 2**). The phenol was treated with propargyl bromide in the presence of K_2CO_3 to yield alkyne (1). Reductive amination of (1) with vanillylamine under basic conditions, followed by acidification, generated amine (2) as the hydrochloride salt. To minimize undesired side reactions in the subsequent alkylation step, the phenolic alcohol of (2) was protected as a tert-butyl-dimethyl-silyl ether to yield (3). Next, (3) was reacted with 8-methylnonanoic acid chloride to form a tertiary amide (4). This was then coupled to PEG_3-BG (5) via CuI-catalyzed click reaction to afford silyl-protected probe (6). Finally, a fluoride-mediated deprotection generated OCT-CAP.

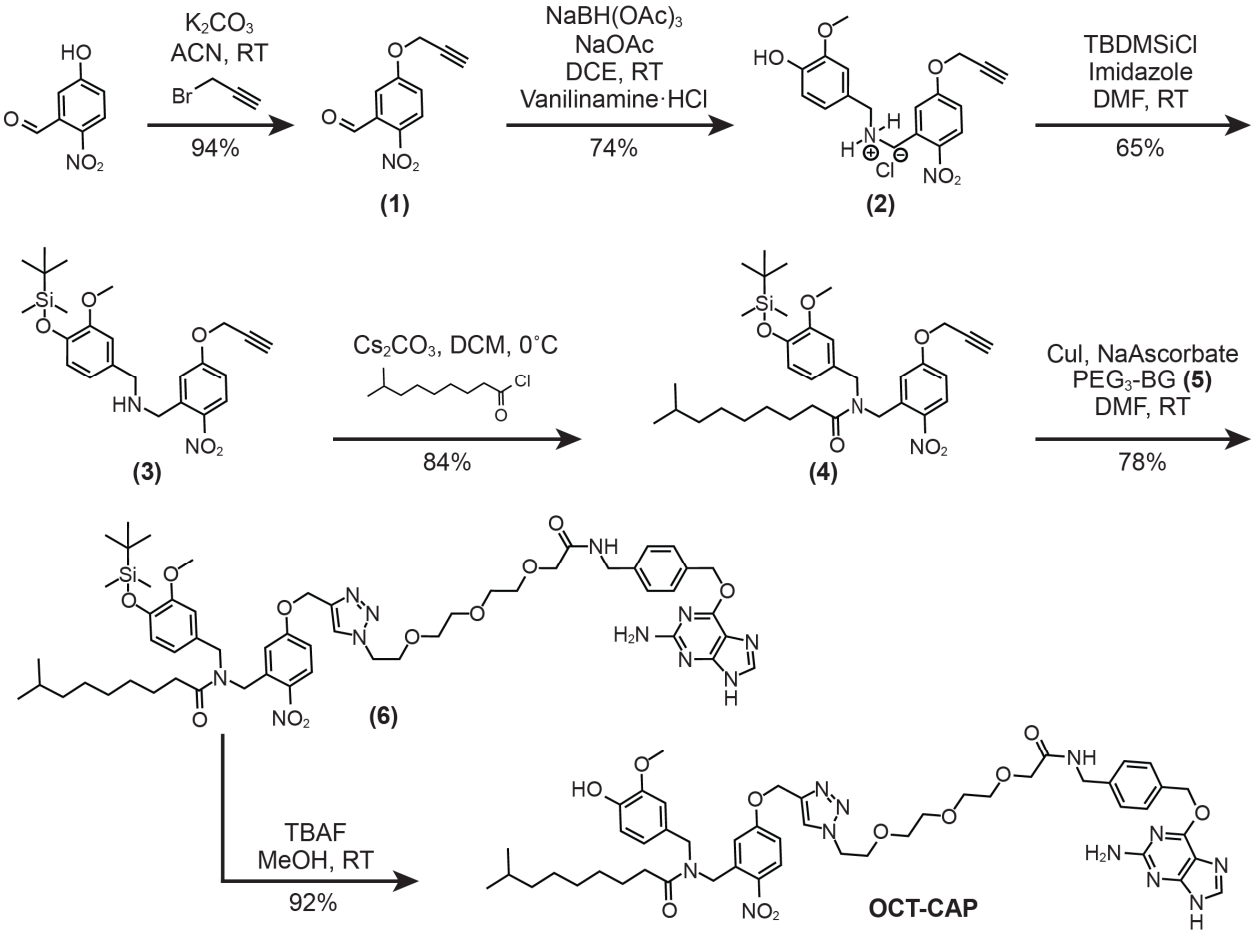

Figure 2. Chemical synthesis of OCT-CAP, which prepared from 5-hydroxy-2-nitrobenzaldehyde in six steps and 27% overall yield.

Photophysical characterization of OCT-CAP by UV-Vis spectroscopy

We used UV-Vis absorbance spectroscopy to characterize the photophysical properties of OCT-CAP. The absorbance spectra of OCT-CAP (20 μM, in DMSO) showed a maximum (λ_{max}) at 287 nm (**Figure 3A**, black). Upon irradiation with 365 nm (~35 mW·cm^{-2}) there was a bathochromic shift of the absorbance spectra and the emergence of a second absorbance peak at 360 nm (**Figure 3A**, red). This result is consistent with the formation of the nitroso-aldehyde photocage byproduct (**Fig. 1B**, bottom right), which has an expanded electronic π-system. We measured OCT-CAP's uncaging kinetics by plotting the absorbance at 360 nm over time (**Figure 3B**). 365 nm illumination triggered uncaging with a τ of 0.6 s. Longer wavelengths—such as 415 nm (purple, ~31 mW·cm^{-2}), 470 nm (blue, ~35 mW·cm^{-2}), and 565 nm (green, ~31 mW·cm^{-2}) did not uncage OCT-CAP, demonstrating that OCT-CAP is only uncaged with UV-A light. This property is advantageous for live-cell microscopy applications, because it allows the probe to be orthogonally uncaged while simultaneously imaging green or red fluorescent biosensors.

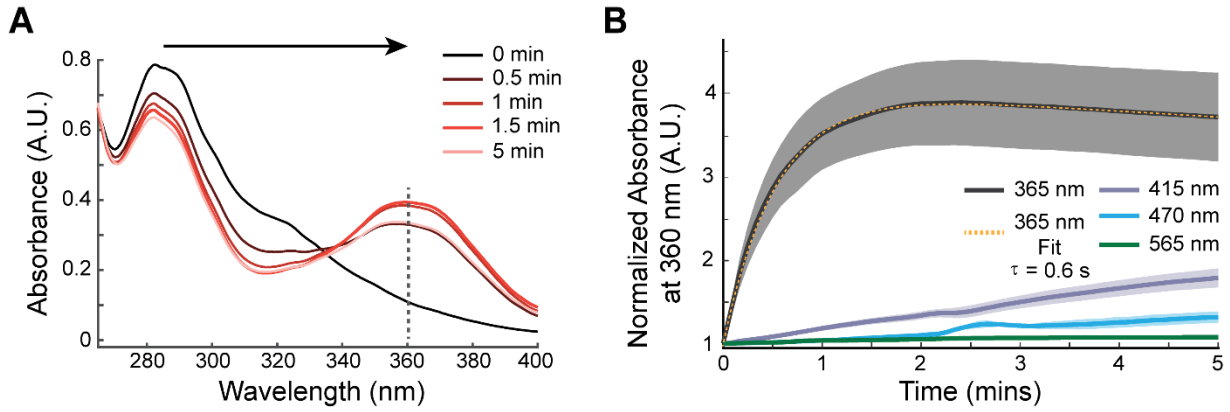

Figure 3. Photophysical characterization of OCT-CAP by UV-Vis spectroscopy. (**A**) The UV-VIS spectra of OCT-CAP (20 μM in DMSO) is plotted over time when illuminated with 365 nm light. A bathochromic shift in the absorbance spectrum was observed as the illumination releases the uncaged product. (**B**) Normalized absorbance of OCT-CAP at 360 nm during irradiation with 365 nm (gray), 415 nm (purple), 470 nm (blue), and 565 nm (green) LEDs. N=3 samples for each condition. Shaded error bars = mean ± SEM.

Tethering OCT-CAP to the surface of TRPV1-expressing HEK293T Cells

Next, we assessed the tethering of OCT-CAP to the surface living cells expressing TRPV1. We transfected HEK293T cells with cDNA encoding TRPV1 with an *N*-terminal YFP (TRPV1-YFP) and SNAP-tags fused to the pDisplay sequence (pDisplay-SNAP), which traffics and anchors the SNAP-tag on the outer cell surface[32]. To confirm that OCT-CAP could covalently attach to the SNAP-tags, we performed a pulse-chase labeling assay between OCT-CAP and a non-permeable JF549i-SNAP dye[33]. HEK293T cells expressing TRPV1-YFP and pDisplay-SNAP were incubated with either a vehicle control (0.1 vol% DMSO) or increasing concentrations of OCT-CAP for 30 or 90 min. The cells were washed with aqueous buffer, then JF549i-SNAP dye was applied to fluorescently label any remaining free SNAP-tags. When pre-incubated with vehicle, JF549i-SNAP dye fluorescence was observed on the perimeters of transfected cells (**Figure 4A**, left), confirming that pDisplay-SNAP is expressed on the outer plasma membrane. Pre-incubation with OCT-CAP blocked JF549i-SNAP labeling in a dose and time-dependent manner, demonstrating that OCT-CAP was indeed tethered to the SNAP-tags (**Figure 4A**, right, **Figure S1**). We found that applying OCT-CAP at 5 μM for 90 min provided complete SNAP-tag labeling on our cell monolayer, which was used as the incubation conditions for the following experiments.

OCT-CAP stimulates Ca^{2+} in TRPV1-expressing HEK293T cells

With OCT-CAP successfully tethered to the surface of TRPV1-expressing HEK293T-cells, we investigated whether uncaging could activate TRPV1 and cause a cellular Ca^{2+} influx. To this end, we performed fluorescent Ca^{2+} imaging using jRGECO1a[34], a Ca^{2+}-sensitive biosensor who's fluorescence increases when cytoplasmic Ca^{2+} levels are elevated. HEK293T cells were transfected with TRPV1-YFP, jRGECO1a, and pDisplay-SNAP, then loaded with OCT-CAP. By confocal microscopy, we observed co-localization between TRPV1, jRGECO1a, and SNAP-tags labeled with JF649 (**Figure 4B**). When irradiated with 375 nm light, there was an increase in jRGECO1a fluorescence, indicating that the intracellular Ca^{2+} concentration in the cells had increased (**Figure 4C**, red; **Figure 4D**). Ionomycin was added at the end of the experiment as a positive control to saturate the jRGECO1a response. Next, we performed several control experiments to verify the biological activity of OCT-CAP and the influence of tethering. First, a vehicle control—i.e., where TRPV1-YFP and pDisplay-SNAP-expressing cells were incubated with DMSO only—resulted in no Ca^{2+} change during 375 nm illumination (**Figure 4C**, black; **Figure 4D**, p=0.001 compared to tethered OCT-CAP). This indicates that exposure to 375 nm

light was not responsible for the Ca^{2+} increase. Next, we repeated tethered OCT-CAP uncaging in cells lacking TRPV1-YFP. Here, probe uncaging did not significantly affect Ca^{2+} levels compared to vehicle control (**Figure 4C**, blue; **Figure 4D**, p=0.2), which confirms that this Ca^{2+} influx was indeed through the overexpressed TRPV1 channels, and not via other ion channels native to HEK293T cells. Finally, we transfected the HEK293T cells an inactive SNAP-tag mutant ($SNAP^{C145A}$) that is unable to tether OCT-CAP[29]. After incubation with OCT-CAP and 375 nm irradiation, the Ca^{2+} increase was comparable to our vehicle control (**Figure 4C**, magenta; **Figure 4D**, p=0.06). This result confirms that OCT-CAP's efficacy is coming from dihydrocapsaicin molecules that are released from the expressed SNAP-tags, as opposed to un-tethered OCT-CAP ligands that had accumulated non-selectively inside or on the cell membrane.

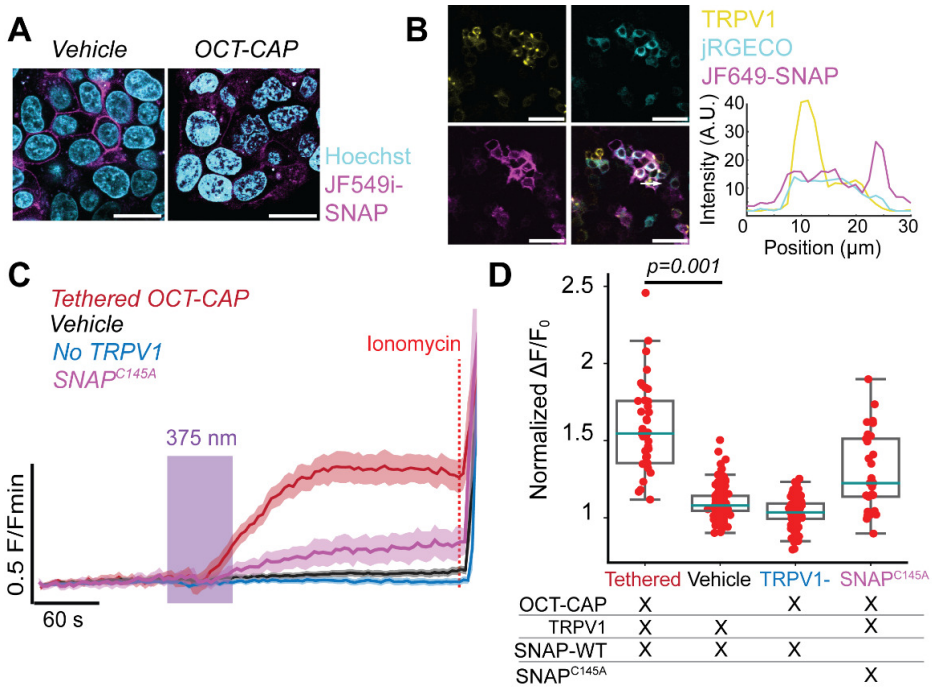

Figure 4. Targeted uncaging of OCT-CAP on HEK293T cells. (**A**) Fluorescence micrographs of live HEK293T cells transfected with pDisplay-SNAP and TRPV1-YFP. In cells labeled with vehicle (0.1 vol% DMSO, 90 min) followed by JF549i-SNAP dye (500 nM, 20 min), JF549i fluorescence was observed on the plasma membrane. In cells labeled with OCT-CAP (5 μM, 90 min) followed by JF549i-SNAP dye, the JF549i fluorescence was abolished. Nuclei were labeled with hoechst-33342 (1 μM, blue). Scale bars are 50 μm. (**B**) Fluorescence colocalization of HEK293T cells expressing TRPV1-YFP (yellow), jRGECO1a (cyan), and pDisplay-SNAP labeled with JF649-SNAP dye (purple). Scale bars are 100 μm. An intensity profile (right) is shown across the white arrow shown in the merged image. (**C**) Fluorescent Ca^{2+} imaging in HEK293T cells transfected with pDisplay-SNAP, TRPV1-YFP, and jRGECO. Average Ca^{2+} traces normalized to baseline pre-irradiation. When tethered OCT-CAP (5 μM, 90 min) was released with 375 nm light, a Ca^{2+} increase was observed (red, N=37, T=4). When the cells were pre-incubated with a vehicle (0.1 vol% DMSO, 90 min) there was no Ca^{2+} increase on irradiation (black, N=137, T=3). When TRPV1 channels were not expressed, there was no effect of irradiation (blue, N=96, T=3). Finally, when transfected with an inactive SNAP-tag mutant (pDisplay-$SNAP^{C145A}$) the Ca^{2+} response induced by OCT-CAP uncaging was greatly attenuated (pink, N=29, T=3). 375 nm irradiation is shown as purple bar. Ionomycin (10 μM) was added at the end of each experiment to saturate jRGECO1a. (**D**) Summary box plot showing the of $\Delta F/F_0$ data from Ca^{2+} imaging trials displayed in C. P-values were calculated using the Student's t-test between biological repeats (T).

OCT-CAP stimulates inward currents in TRPV1-Expressing HEK293T Cells

Next, we characterized OCT-CAP's activity in TRPV1-expressing cells using electrophysiology. HEK293T cells were transfected with pDisplay-SNAP and TRPV1-YFP. We charged the cells with OCT-CAP, washed with extracellular buffer, then recorded whole-cell currents in voltage clamp mode. During the irradiation, we observed a large inward current, indicating that TRPV1 had been activated (**Figure 5A,B**). Subsequent wash-on of CAP after photoactivation did not increase the current, and the OCT-CAP inward current was similar in magnitude to when CAP was washed-on to the cells alone (**Figure S2A**). These results indicate that TRPV1 was fully activated by OCT-CAP uncaging. The current response from incubated OCT-CAP was dose-dependent, and first observable with a 5 μM concentration (**Figure S2B**). Incubation with OCT-CAP at lower concentrations exhibit no inward current, which is in line with our previously-described fluorescence labeling results (**Figure S1**). HEK293T cells that lacked TRPV1-YFP (i.e., pDisplay-SNAP only) did not respond to OCT-CAP, confirming that OCT-CAP is selective for the heterologously expressed TRPV1 channels, and did not arise from other channels native to the HEK293T cells (**Figure 5B**, **Figure S2C**). Additionally, we added the TRPV1 antagonist capsazepine (CPZ) to our external buffer. In the presence of CPZ, the inward current caused by tethered OCT-CAP uncaging was significantly decreased (**Figure 5B**, **Figure S2D**); again, confirming that OCT-CAP was selective for the expressed TRPV1 ion channels. We did not observe UV-A-triggered currents in TRPV1-YFP and pDisplay-SNAP-expressing cells exposed only to a vehicle (**Figure 5B**, **Figure S2E**), confirming that the observed TRPV1 currents were not caused by the UV-A irradiation. In HEK293T cells expressing the inactive $SNAP^{C145A}$ mutant, there was no change in current upon UV-A (**Figure 5B,C**); again, confirming that the current response was driven by OCT-CAP molecules tethered to the cell surface.

Finally, we aimed to demonstrate the utility of tethered OCT-CAP in comparison to the freely-diffusible photocage. We applied OCT-CAP to the external buffer, then recorded and uncaged immediately, without giving the probe time to be enriched by the SNAP-tags. In this case, UV-A irradiation produced only a small inward current (**Figure 5B,D**). This was significantly smaller when compared to tethered OCT-CAP uncaging ($p=0.03$), and not significantly different compared to our vehicle control ($p=0.2$). CAP wash-on at the end of the experiment resulted in a large inward current, demonstrating that untethered OCT-CAP uncaging did not fully activate all the TRPV1 channel expressed on the patched cell. This result highlights that that enrichment of OCT-CAP at the cell surface increases our photocage's efficacy compared to having the freely diffusing photocaged CAP present in the bath.

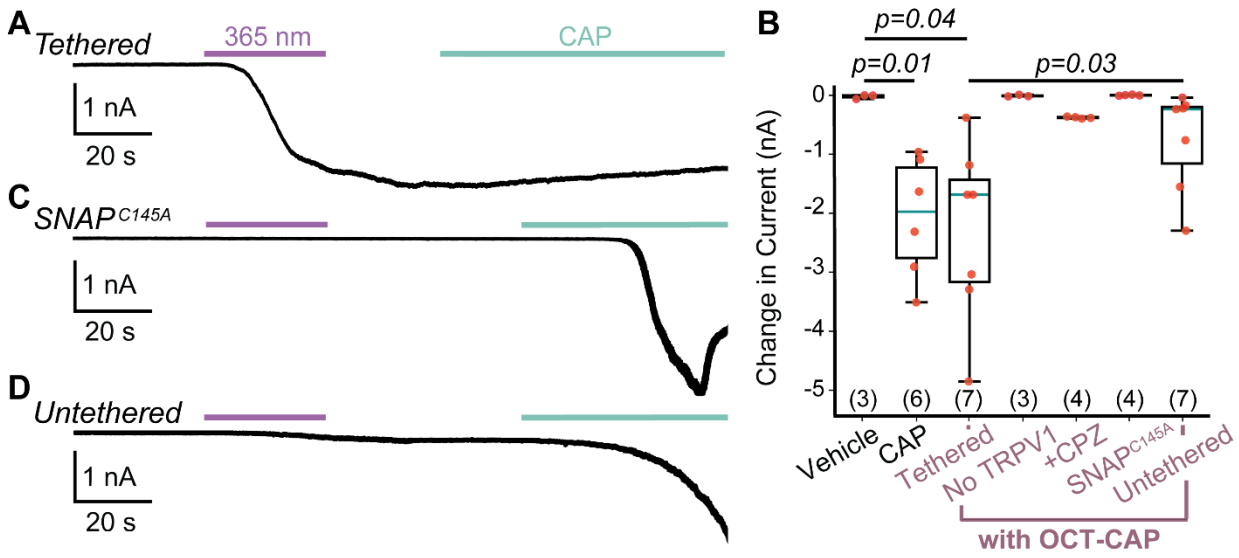

Figure 5. Targeted uncaging of OCT-CAP on HEK293T cells measured by electrophysiology. Whole-cell voltage-clamp electrophysiology on HEK293T cells expressing TRPV1-YFP and pDisplay-SNAP, then loaded with OCT-CAP (5 μM) or vehicle (0.1 vol% DMSO) for 90 min. (**A**) Representative time series trace of current induced by OCT-CAP upon 365 nm UV-A irradiation. CAP (5 μM) addition at the end of the experiment did not increase the current further. (**B**) Box plot summary of current changes induced by UV-A irradiation under various ligand incubation and transfection conditions. The number of cells (N) is included in brackets under each box. P-values were calculated using the Student's t-test. (**C**) Representative time series trace of current induced by OCT-CAP upon UV-A irradiation when expressing the inactive SNAP^{C145A} mutant. No response is observed for OCT-CAP uncaging, but CAP causes a large inward current. (**D**) When OCT-CAP (5 μM) was added to the external buffer but not given time to tether to the SNAP-tags, UV-A irradiation produced only a small inward current, which could be greatly potentiated by perfusion of CAP.

DISCUSSION

This study presents the expansion of OCT-ligand technology to target TRPV1 ion channels on genetically defined cellular membranes. Our new probe, OCT-CAP, is a photocaged capsaicin analog that can be tethered to membrane-anchored SNAP-tags. We showed that enriching and uncaging OCT-CAP on the plasma membrane enables rapid TRPV1 activation after agonist uncaging with UV-light, and provides superior TRPV1 activation potency when compared to a freely diffusible photocage applied in the external buffer. OCT-CAP responds to UV-A light, so it can be combined with other green/red fluorescent biosensors (e.g., for Ca^{2+} or cAMP) in live-cell imaging applications. Another practical advantage of this tool is that it eliminates the need for an external perfusion system. Gravity-based perfusion systems provide slow kinetics as the ligand solution must replace the external bath solution surrounding the cells. This effect is especially detrimental when working with hydrophobic ligands, such as CAP, which stick to tubing and precipitate out of physiological solutions. When using OCT-CAP, the ligand can simply be pre-loaded onto the cells, and the probe is activated on-demand without the use of any perfusion system; this greatly eases the experimental setup when working with these lipid agonists.

While other approaches have used membrane-bound SNAP tags to tether receptor ligands and photoswitches to cells or membranes of interest[35,36], these are limited by the fact that the ligand always remains attached to the linker. The OCT-ligand approach avoids this disadvantage by releasing the unmodified ligand; and as such, can be used to study the downstream physiology of endogenous signaling molecules and their receptors. The scope of potential targets extends beyond fatty acid amides like CAP or endocannabinoids. OCT-ligands for the targeted photo-release of other lipids such as fatty acids, diacylglycerols, or even neurotransmitters like serotonin and dopamine will allow a variety of endogenous signaling pathways to be interrogated with optogenetic precision.

The current set of OCT-ligands have only been applied at the cell surface. In part, this is due to the surface-expression of our receptor targets so far (TRPV1 and GPR55[29]), alongside the PEG-moiety embedded within OCT-CAP's linker, which prevents it from readily crossing membranes. As such, a future area of OCT-ligand development will be their targeting to intracellular compartments. Several studies have suggested that TRPV1 can be expressed on internal membranes such as the endoplasmic reticulum[37,38]; and so far, no tools exist to selectively activate these internal receptor pools. Future-studies using cell-permeable OCT-CAP derivatives, alongside SNAP-tags directed to intracellular membranes, will help us understand the roles of these understudied intracellular pathways. Another area of future development will

be towards multiplexed stimulation. As our repertoire of OCT-ligands expands in terms of ligands and biological targets, multiple probes can be used in combination by applying orthogonal bio-conjugation tags—e.g., Halo[26] or CLIP[28]-tags. This could allow us to deliver complex stimulation patterns sets of receptor agonist/antagonist pairs, and will allow us to dissect signaling pathways in a more sophisticated manner than is currently possible.

In summary, this work describes the expansion of OCT-ligand tethered photopharmacology to control ion channel activity, and sets the stage for optical control over a diverse set of biological targets. We envision that the next generation of OCT-ligands will be broadly applicable tools for studying the function of lipids in a variety of experimental applications, and will help us unravel the intricate signaling networks that exist within distinct organelles, cell types and tissues.

AUTHOR CONTRIBUTIONS

J.A.F. conceived and coordinated the study. D.I.A. synthesized and characterized the compound. C.L.H. performed UV-VIS, fluorescence imaging, and electrophysiology experiments. C.L.H., D.I.A, and J. A. F. wrote the manuscript. C.L.H. and D.I.A. contributed equally to this project, and either has the right to list themselves first in bibliographic documents.

ACKNOWLEDGEMENTS

The authors thank Dr. Carsten Schultz for providing microscopy resources. We also thank Dr. Janelle Tobias and Alexander Viray for input on this study. This work was funded in part by the Burroughs Wellcome Fund Career Award at the Scientific Interface (to C.L.H., 1013313).

CONFLICTS OF INTEREST

There are no conflicts to declare.

REFERENCES

(1) Caterina, M. J.; Schumacher, M. A.; Tominaga, M.; Rosen, T. A.; Levine, J. D.; Julius, D. The Capsaicin Receptor: A Heat-Activated Ion Channel in the Pain Pathway. *Nature* **1997**, *389* (6653), 816–824. https://doi.org/10.1038/39807.

(2) Jardín, I.; López, J. J.; Diez, R.; Sánchez-Collado, J.; Cantonero, C.; Albarrán, L.; Woodard, G. E.; Redondo, P. C.; Salido, G. M.; Smani, T.; Rosado, J. A. TRPs in Pain Sensation. *Front. Physiol.* **2017**, *8*, 392. https://doi.org/10.3389/fphys.2017.00392.

(3) Hurtado-Zavala, J. I.; Ramachandran, B.; Ahmed, S.; Halder, R.; Bolleyer, C.; Awasthi, A.; Stahlberg, M. A.; Wagener, R. J.; Anderson, K.; Drenan, R. M.; Lester, H. A.; Miwa, J. M.; Staiger, J. F.; Fischer, A.; Dean, C. TRPV1 Regulates Excitatory Innervation of OLM Neurons in the Hippocampus. *Nat. Commun.* **2017**, *8* (1), 15878. https://doi.org/10.1038/ncomms15878.

(4) Balleza-Tapia, H.; Crux, S.; Andrade-Talavera, Y.; Dolz-Gaiton, P.; Papadia, D.; Chen, G.; Johansson, J.; Fisahn, A. TrpV1 Receptor Activation Rescues Neuronal Function and Network Gamma Oscillations from Aβ-Induced Impairment in Mouse Hippocampus in Vitro. *eLife* **2018**, *7*, e37703. https://doi.org/10.7554/eLife.37703.

(5) Razavi, R.; Chan, Y.; Afifiyan, F. N.; Liu, X. J.; Wan, X.; Yantha, J.; Tsui, H.; Tang, L.; Tsai, S.; Santamaria, P.; Driver, J. P.; Serreze, D.; Salter, M. W.; Dosch, H.-M. TRPV1+ Sensory Neurons Control β Cell Stress and Islet Inflammation in Autoimmune Diabetes. *Cell* **2006**, *127* (6), 1123–1135. https://doi.org/10.1016/j.cell.2006.10.038.

(6) Bae, C.; Anselmi, C.; Kalia, J.; Jara-Oseguera, A.; Schwieters, C. D.; Krepkiy, D.; Won Lee, C.; Kim, E.-H.; Kim, J. I.; Faraldo-Gómez, J. D.; Swartz, K. J. Structural Insights into the Mechanism of Activation of the TRPV1 Channel by a Membrane-Bound Tarantula Toxin. *eLife* **2016**, *5*, e11273. https://doi.org/10.7554/eLife.11273.

(7) Geron, M.; Hazan, A.; Priel, A. Animal Toxins Providing Insights into TRPV1 Activation Mechanism. *Toxins* **2017**, *9* (10), 326. https://doi.org/10.3390/toxins9100326.

(8) Dhaka, A.; Uzzell, V.; Dubin, A. E.; Mathur, J.; Petrus, M.; Bandell, M.; Patapoutian, A. TRPV1 Is Activated by Both Acidic and Basic pH. *J. Neurosci.* **2009**, *29* (1), 153–158. https://doi.org/10.1523/JNEUROSCI.4901-08.2009.
(9) Fenwick, A. J.; Fowler, D. K.; Wu, S. W.; Shaffer, F. J.; Lindberg, J. E. M.; Kinch, D. C.; Peters, J. H. Direct Anandamide Activation of TRPV1 Produces Divergent Calcium and Current Responses. *Front. Mol. Neurosci.* **2017**, *10*. https://doi.org/10.3389/fnmol.2017.00200.
(10) Broichhagen, J.; Frank, J. A.; Trauner, D. A Roadmap to Success in Photopharmacology. *Acc. Chem. Res.* **2015**, *48* (7), 1947–1960. https://doi.org/10.1021/acs.accounts.5b00129.
(11) Stein, M.; Breit, A.; Fehrentz, T.; Gudermann, T.; Trauner, D. Optical Control of TRPV1 Channels. *Angew. Chem. Int. Ed.* **2013**, *52* (37), 9845–9848. https://doi.org/10.1002/anie.201302530.
(12) Frank, J. A.; Moroni, M.; Moshourab, R.; Sumser, M.; Lewin, G. R.; Trauner, D. Photoswitchable Fatty Acids Enable Optical Control of TRPV1. *Nat. Commun.* **2015**, *6* (1), 7118. https://doi.org/10.1038/ncomms8118.
(13) Konrad, D. B.; Frank, J. A.; Trauner, D. Synthesis of Redshifted Azobenzene Photoswitches by Late-Stage Functionalization. *Chem. Eur. J.* **2016**, *22* (13), 4364–4368.
(14) Frank, J. A.; Antonini, M. J.; Chiang, P. H.; Canales, A.; Konrad, D. B.; Garwood, I. C.; Rajic, G.; Koehler, F.; Fink, Y.; Anikeeva, P. In Vivo Photopharmacology Enabled by Multifunctional Fibers. *ACS Chem. Neurosci.* **2020**, *11* (22), 3802–3813. https://doi.org/10.1021/acschemneuro.0c00577.
(15) Klán, P.; Šolomek, T.; Bochet, C. G.; Blanc, A.; Givens, R.; Rubina, M.; Popik, V.; Kostikov, A.; Wirz, J. Photoremovable Protecting Groups in Chemistry and Biology: Reaction Mechanisms and Efficacy. *Chem. Rev.* **2013**, *113* (1), 119–191. https://doi.org/10.1021/cr300177k.
(16) Katritzky, A. R.; Xu, Y.-J.; Vakulenko, A. V.; Wilcox, A. L.; Bley, K. R. Model Compounds of Caged Capsaicin: Design, Synthesis, and Photoreactivity. *J. Org. Chem.* **2003**, *68* (23), 9100–9104. https://doi.org/10.1021/jo034616t.
(17) Zemelman, B. V.; Nesnas, N.; Lee, G. A.; Miesenböck, G. Photochemical Gating of Heterologous Ion Channels: Remote Control over Genetically Designated Populations of Neurons. *Proc. Natl. Acad. Sci.* **2003**, *100* (3), 1352–1357. https://doi.org/10.1073/pnas.242738899.
(18) Carr, J. L.; Wease, K. N.; Van Ryssen, M. P.; Paterson, S.; Agate, B.; Gallagher, K. A.; Brown, C. T. A.; Scott, R. H.; Conway, S. J. In Vitro Photo-Release of a TRPV1 Agonist. *Bioorg. Med. Chem. Lett.* **2006**, *16* (1), 208–212. https://doi.org/10.1016/j.bmcl.2005.09.018.
(19) Zhao, J.; Gover, T. D.; Muralidharan, S.; Auston, D. A.; Weinreich, D.; Kao, J. P. Y. Caged Vanilloid Ligands for Activation of TRPV1 Receptors by 1- and 2-Photon Excitation. *Biochemistry* **2006**, *45* (15), 4915–4926. https://doi.org/10.1021/bi052082f.
(20) Gilbert, D.; Funk, K.; Dekowski, B.; Lechler, R.; Keller, S.; Möhrlen, F.; Frings, S.; Hagen, V. Caged Capsaicins: New Tools for the Examination of TRPV1 Channels in Somatosensory Neurons. *ChemBioChem* **2007**, *8* (1), 89–97. https://doi.org/10.1002/cbic.200600437.
(21) Ellis-Davies, G. C. R. Caged Compounds: Photorelease Technology for Control of Cellular Chemistry and Physiology. *Nat. Methods* **2007**, *4* (8), 619–628. https://doi.org/10.1038/nmeth1072.
(22) Boyden, E. S.; Zhang, F.; Bamberg, E.; Nagel, G.; Deisseroth, K. Millisecond-Timescale, Genetically Targeted Optical Control of Neural Activity. *Nat. Neurosci.* **2005**, *8* (9), 1263–1268. https://doi.org/10.1038/nn1525.
(23) Güler, A. D.; Rainwater, A.; Parker, J. G.; Jones, G. L.; Argilli, E.; Arenkiel, B. R.; Ehlers, M. D.; Bonci, A.; Zweifel, L. S.; Palmiter, R. D. Transient Activation of Specific Neurons in

Mice by Selective Expression of the Capsaicin Receptor. *Nat. Commun.* **2012**, *3* (1), 746. https://doi.org/10.1038/ncomms1749.
(24) Roth, B. L. DREADDs for Neuroscientists. *Neuron* **2016**, *89* (4), 683–694. https://doi.org/10.1016/j.neuron.2016.01.040.
(25) Keppler, A.; Gendreizig, S.; Gronemeyer, T.; Pick, H.; Vogel, H.; Johnsson, K. A General Method for the Covalent Labeling of Fusion Proteins with Small Molecules in Vivo. *Nat. Biotechnol.* **2003**, *21* (1), 86–89. https://doi.org/10.1038/nbt765.
(26) Los, G. V.; Encell, L. P.; McDougall, M. G.; Hartzell, D. D.; Karassina, N.; Zimprich, C.; Wood, M. G.; Learish, R.; Ohana, R. F.; Urh, M.; Simpson, D.; Mendez, J.; Zimmerman, K.; Otto, P.; Vidugiris, G.; Zhu, J.; Darzins, A.; Klaubert, D. H.; Bulleit, R. F.; Wood, K. V. HaloTag: A Novel Protein Labeling Technology for Cell Imaging and Protein Analysis. *ACS Chem. Biol.* **2008**, *3* (6), 373–382. https://doi.org/10.1021/cb800025k.
(27) England, C. G.; Luo, H.; Cai, W. HaloTag Technology: A Versatile Platform for Biomedical Applications. *Bioconjug. Chem.* **2015**, *26* (6), 975–986. https://doi.org/10.1021/acs.bioconjchem.5b00191.
(28) Gautier, A.; Juillerat, A.; Heinis, C.; Corrêa, I. R.; Kindermann, M.; Beaufils, F.; Johnsson, K. An Engineered Protein Tag for Multiprotein Labeling in Living Cells. *Chem. Biol.* **2008**, *15* (2), 128–136. https://doi.org/10.1016/j.chembiol.2008.01.007.
(29) Tobias, J. M.; Rajic, G.; Viray, A. E. G.; Icka-Araki, D.; Frank, J. A. Genetically-Targeted Photorelease of Endocannabinoids Enables Optical Control of GPR55 in Pancreatic β-Cells. *Chem. Sci.* **2021**, *12* (40), 13506–13512. https://doi.org/10.1039/d1sc02527a.
(30) Nelson, E. K.; Dawson, L. E. THE CONSTITUTION OF CAPSAICIN, THE PUNGENT PRINCIPLE OF CAPSICUM. III. *J. Am. Chem. Soc.* **1923**, *45* (9), 2179–2181. https://doi.org/10.1021/ja01662a023.
(31) Walpole, C. S. J.; Wrigglesworth, R.; Bevan, S.; Campbell, E. A.; Dray, A.; James, I. F.; Masdin, K. J.; Perkins, M. N.; Winter, J. Analogs of Capsaicin with Agonist Activity as Novel Analgesic Agents; Structure-Activity Studies. 3. The Hydrophobic Side-Chain "C-Region." *J. Med. Chem.* **1993**, *36* (16), 2381–2389. https://doi.org/10.1021/jm00068a016.
(32) Puttikhunt, C.; Kasinrerk, W.; Srisa-ad, S.; Duangchinda, T.; Silakate, W.; Moonsom, S.; Sittisombut, N.; Malasit, P. Production of Anti-Dengue NS1 Monoclonal Antibodies by DNA Immunization. *J. Virol. Methods* **2003**, *109* (1), 55–61. https://doi.org/10.1016/S0166-0934(03)00045-4.
(33) Grimm, J. B.; Muthusamy, A. K.; Liang, Y.; Brown, T. A.; Lemon, W. C.; Patel, R.; Lu, R.; Macklin, J. J.; Keller, P. J.; Ji, N.; Lavis, L. D. A General Method to Fine-Tune Fluorophores for Live-Cell and in Vivo Imaging. *Nat. Methods* **2017**, *14* (10), 987–994. https://doi.org/10.1038/nmeth.4403.
(34) Dana, H.; Mohar, B.; Sun, Y.; Narayan, S.; Gordus, A.; Hasseman, J. P.; Tsegaye, G.; Holt, G. T.; Hu, A.; Walpita, D.; Patel, R.; Macklin, J. J.; Bargmann, C. I.; Ahrens, M. B.; Schreiter, E. R.; Jayaraman, V.; Looger, L. L.; Svoboda, K.; Kim, D. S. Sensitive Red Protein Calcium Indicators for Imaging Neural Activity. *eLife* **2016**, *5*, e12727. https://doi.org/10.7554/eLife.12727.
(35) Shields, B. C.; Kahuno, E.; Kim, C.; Apostolides, P. F.; Brown, J.; Lindo, S.; Mensh, B. D.; Dudman, J. T.; Lavis, L. D.; Tadross, M. R. Deconstructing Behavioral Neuropharmacology with Cellular Specificity. *Science* **2017**, *356* (6333), eaaj2161. https://doi.org/10.1126/science.aaj2161.
(36) Donthamsetti, P. C.; Broichhagen, J.; Vyklicky, V.; Stanley, C.; Fu, Z.; Visel, M.; Levitz, J. L.; Javitch, J. A.; Trauner, D.; Isacoff, E. Y. Genetically Targeted Optical Control of an Endogenous G Protein-Coupled Receptor. *J. Am. Chem. Soc.* **2019**, *141* (29), 11522–11530. https://doi.org/10.1021/jacs.9b02895.
(37) Gavva, N. R.; Klionsky, L.; Qu, Y.; Shi, L.; Tamir, R.; Edenson, S.; Zhang, T. J.; Viswanadhan, V. N.; Toth, A.; Pearce, L. V.; Vanderah, T. W.; Porreca, F.; Blumberg, P. M.;

Lile, J.; Sun, Y.; Wild, K.; Louis, J.-C.; Treanor, J. J. S. Molecular Determinants of Vanilloid Sensitivity in TRPV1. *J. Biol. Chem.* **2004**, *279* (19), 20283–20295. https://doi.org/10.1074/jbc.M312577200.

(38) Smutzer, G.; Devassy, R. K. Integrating TRPV1 Receptor Function with Capsaicin Psychophysics. *Adv. Pharmacol. Sci.* **2016**, *2016*, 1–16. https://doi.org/10.1155/2016/1512457.